THE CO-CURE OF HONEYCOMB SANDWICH STRUCTURES: PROCESS PHYSICS AND MANUFACTURING STRATEGIES

Timotei Centea[1], Mark Anders[2], Daniel Zebrine[3], and Steven Nutt[4]

[1,2,3,4]M.C. Gill Composites Center, Viterbi School of Engineering, University of Southern California
3651 Watt Way, VHE-406, Los Angeles, California, United States of America
Email: [1]centea@usc.edu, [2]anders@usc.edu, [3]zebrine@usc.edu, [4]nutt@usc.edu
Web Page: http://composites.usc.edu

Keywords: Honeycomb, Sandwich, Processing, Prepreg, Defects

Abstract
The co-cure of honeycomb sandwich structures involves complex physical phenomena and poses challenges for manufacturing process development. This paper describes results from a multi-year research project on co-cure, during which *in situ* observations, processing trials, and microstructural analysis were used to understand key physics and defect formation mechanisms. Results show that co-cure is governed by interactions between core pressure evolution, bond-line formation, and facesheet consolidation, and that defect evolution is path-dependent and challenging to control. However, results also demonstrate a manufacturing strategy for successful and reliable co-cure. Overall, the paper clarifies the fundamental science associated with co-cure of honeycomb sandwich structures, and provides a viable pathway for optimizing manufacturing processes.

1. Introduction

Honeycomb sandwich structures consist of two fiber-reinforced laminate facesheets bonded using adhesive to a lightweight core. Sandwich construction is ubiquitous in aerospace (and elsewhere) because it offers high specific mechanical properties and design versatility.The facesheets carry tensile and compressive loads, the core resists shear and stiffens the structure by distancing the facesheets from the neutral axis, and the adhesive transfers loads between constituents. Honeycomb panels can be "co-cured" by performing facesheet consolidation (from prepreg plies) and adhesive bonding (using film adhesive) in a single step. Co-cure is preferable to post-cure bonding because it eliminates fitment issues, enabling production of complex geometries, and can be performed in a single step. However, co-cure is technically challenging. Material compatibility is required to cure prepreg and adhesive at the same time, and complex interactions between constituents often lead to higher defect levels than those achievable in monolithic laminates. As such, despite frequent use of sandwich structures, developing successful co-cure processes remains a persistent problem in composites manufacturing.

The physics of co-cure can be divided into three categories: facesheet consolidation, adhesive bond-line formation, and core pressure evolution. Literature on composites processing science has addressed many relevant aspects of these phenomena, including prepreg consolidation over monolithic tooling (e.g., [1,2]) and adhesive behavior. However, the major challenges of co-cure reside in complex interactions between prepeg, adhesive, and core. Recently, two research efforts have investigated co-cure of honeycomb structures in the context of out-of-autoclave/vacuum bag-only (OoA/VBO) processing. Tavares et al. [3,4,5,6,7] analyzed the through-thickness permeability of prepreg-adhesive skins before and during cure, as well as the influence of the resulting core pressure evolution on microstructural quality and mechanical performance. Kratz et al. [8,9,10,11,12,13,14] subsequently expanded upon these studies by exploring relationships between material characteristics and process physics, high-

lighting the significant variability inherent in core gas transport, and employing *in situ* measurements and modeling to analyze the evolution of core pressure as a function of thermal expansion, gas transport, and moisture volatilization. Together, these investigations emphasized that successful co-cure (or defect formation) is contingent upon the interaction between the evolving core pressure and the facesheet-adhesive "skin." However, both series of studies are limited by their focus on OoA/VBO processing, which constrains process pressures to a subset of those achievable using traditional autoclave co-cure. Other published literature provides useful evidence of causal relationships between material, process, and quality (e.g., [15,16]). However, stand-alone studies of co-cure are inherently anecdotal, with results potentially limited to specific materials or process conditions. Thus, despite valuable prior studies, no comprehensive understanding of co-cure has yet been developed.

This paper describes major findings from a multi-year project focused on understanding and modeling the co-cure of honeycomb sandwich structures. Specifically, we focus on outlining methodologies developed to analyze the governing physics of co-cure, and on describing experimental results that clarify the process physics, highlight potential defect formation mechanisms, and demonstrate a viable strategy for successful co-cure of parts with low defect levels. To expand upon prior studies, we define co-cure as an autoclave process during which temperature (T), autoclave pressure (P_a), and bag pressure (P_b) are controllable. Furthermore, we distinguish between two cases of core pressure (P_c) evolution. During *equilibrated* co-cure, the bag and core gas volumes are directly connected, such that $P_c = P_b$. Such situations may arise, for example, during fabrication of aircraft engine nacelles, as a bag-side skin is co-cured while a pre-cured and perforated tool-side skin is bonded to the core. Conversely, during co-cure with *sealed* core, the core gas pressure evolves in a non-linear manner, subject to thermal expansion, gas transport through skins, and volatile release from core and polymers.

2. Materials and Methods

The materials used to generate data presented in this paper consisted of aerospace-grade prepregs, film adhesives, and core. The prepreg comprised a plain weave carbon fiber fabric and thermoset epoxy resin (Hexcel HexPly® 8552S, ACP-PW reinforcement with areal weight of 193 g/m^2). The film adhesive was made from a thermoset epoxy resin (Cytec Solvay FM 309-1M0.5 in a supported variant). Honeycomb core inserts consisted of a Nomex material (Gill Corporation GillCore, with density of 48 kg/m^3 and cell sizes of 3.175 mm or 6.35 mm, respectively). Other prepreg and adhesive materials were studied, but are omitted from this paper due to length limitations. The influence of non-structural ancillary materials (e.g., lightweight scrims) has not yet been assessed.

Experiments were conducted to clarify underlying physics and defect formation mechanisms. Lab-scale process analysis methods were developed: (1) to replicate, in an accurate but controlled manner, industrial processing conditions, and (2) to overcome the "black box" nature of autoclave cure through *in situ* visualization and real-time measurement of process phenomena.

Figure 1 shows an instrumented co-cure analysis fixture [17]. The main component consisted of a tool plate (280 × 280 mm) with an integrated pocket (76 × 76 × 19 mm), which contained one (or more) glass spacers and a transparent window. The tool surface was used to lay up prepreg plies and film adhesive (sized larger than the pocket), while the core insert was placed into the pocket, forming the bag-side half of a sandwich assembly. The glass spacer and window enabled direct observation of the bond-line, while a vacuum bag was assembled on the tool surface using standard consumables. Finally, a solid lid was attached to the tool plate to form a sealed, autoclave-like environment outside the vacuum bag. The autoclave, bag, and core pressures were independently measured using integrated transducers and controlled (if desired) using dedicated ports. A melt pressure sensor was also mounted (recessed by 6.35 mm) onto the tool plate to measure resin pressure within the prepreg edge-band. The tool plate and lid were equipped with stand-alone heating systems. Altogether, this "mini-autoclave" accurately replicated autoclave cure conditions while enabling detailed diagnostics of process physics.

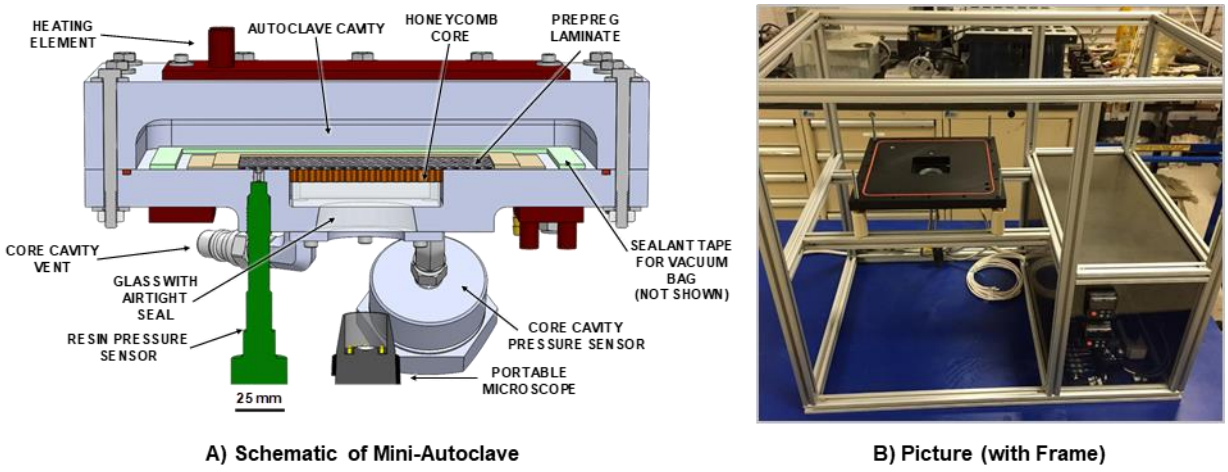

Figure 1: (A) Schematic of mini-autoclave fixture, and (B) picture of test fixture with support frame

The mini-autoclave was used to perform over one hundred tests with diverse material and process configurations. Tests with controlled and constant P_a, P_b, and P_c were conducted to study physical phenomena in simple isobaric conditions, reflecting co-cure under equilibrated conditions. Alternately, P_c was allowed to evolve to study process phenomena in conditions representative of co-cured with sealed core. For all tests, the layup sequence consisted of placing the honeycomb insert, film adhesive, and prepreg plies, and overlaying these consitutents with a perforated release film, a layer of breather, and a vacuum bag membrane. Sealant tape was used to close off the bag, and to form either breathing (permeable) or sealing (non-permeable) edge dams for the facesheet, depending on test requirements. For this paper, the thermal cycle consisted of a room-temperature vacuum hold (0 – 60 min, depending on the test) followed by a two-step profile with dwells at 110°C (60 min) and 177°C (120 min), and with 2°C/min ramps. Pressure cycles differed between tests, as explained above. However, in all cases, the consolidation pressure (P_a - P_b) exceeded P_c, eliminating risk of skin-core delaminations. The mini-autoclave can also be used to characterize specific physical phenomena (e.g., the permeability of the facesheets to gases), as detailed elsewhere [17,18].

3. Results and Discussion

3.1. *In Situ* Observation of Co-Cure Physics

Figure 2 and 3 show representative results from a co-cure experiment during which a four-ply prepreg facesheet and a single layer of film adhesive (unsupported) were co-cured over Nomex core (6.35 mm cells). The adhesive was reticulated (selectively dewetted onto core walls by perforation and local heating) prior to co-cure, to enable observation of prepreg surfaces. The cure cycle consisted of a one-hour room-temperature vacuum hold followed by the thermal profile described in Section 2.3. The bag pressure was set to vacuum throughout co-cure. The autoclave pressure was raised to P_a = 377 kPa (40 psig) at the onset of heating. Results from this experiment illustrate key co-cure phenomena. Figure 2 shows measured temperature and pressure traces. The evolution of core pressure versus time and other process parameters is specifically important. During the room temperature hold, P_c decreased when bag vacuum was imposed (because of pre-existing egress pathways in the prepreg and at interfaces), stabilized for 50 min (once the egress pathways were closed off by compaction), and decreased once again prior to application of heat and autoclave pressure (likely due to formation of channels within the uncured prepreg). Subsequently, the core pressure increased with heat-up (because of thermal expansion and moisture release from the core) but decreased during dwells (due to air evacuation through the curing facesheets). Overall, this core pressure trace shows the complex possible interactions between materials and process factors during co-cure.

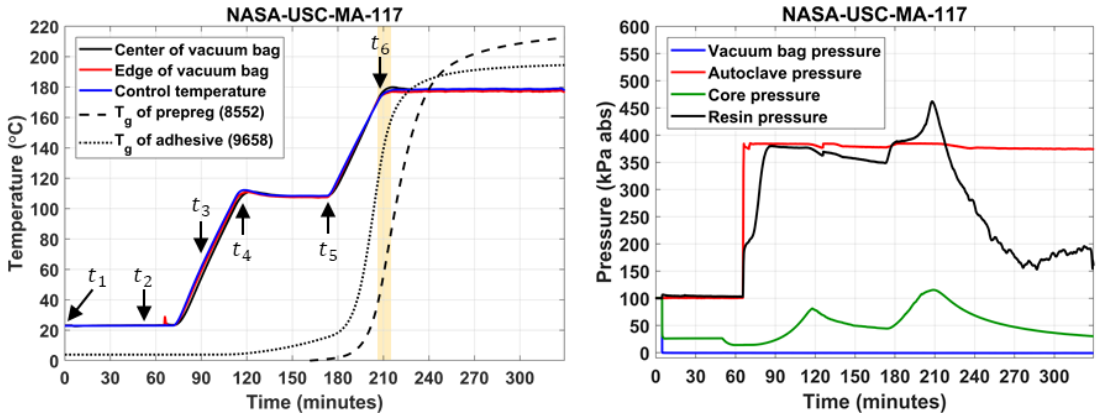

Figure 2: (A) Temperature and (B) pressure data, with gelation shown as shaded. The resin pressure exceeds P_a after gelation because of thermal expansion of a pressure-transfer fluid.

Figure 3 shows video micrographs of the evolving bond-line at different stages of co-cure ($t_1 - t_6$). The first image (t_1 = 0 min) shows the bond-line in its initial, as-laid condition, with adhesive located at the top of the cell walls and a resin-rich prepreg surface atop the cells. No voids are visible. The second image (t_2 = 50 min) shows evidence of air migration into the core, including bubbles at pinholes of the woven fabric and in adhesive located over the pinholes, suggesting that the pressure of resin and air entrapped between prepreg plies exceeded P_c. At t_3 = 90 min, adhesive flow led to fillets (menisci) at core/skin interfaces. Furthermore, the prepreg resin surrounding the pinholes was filled with clusters of voids. At t_4 = 117 min, the end of initial heat-up and a peak in P_c, the fillets grew larger, but prepreg resin voids were suppressed by the rising core pressure. Porosity remained visible within the adhesive, possibly due to thinning at fillet edges. At t_5 = 172 min, by the end of the first dwell, porosity is visible within both prepreg and adhesive due to a decrease in P_c from the preceding peak. Finally, at t_6 = 209 min, at the end of the second heat-up ramp, significant porosity is visible within the prepreg resin, with some voids also present in the adhesive. The void levels observed at this point are attributed to temperature-driven diffusion and pressurization, despite the highest P_c measured during the cycle.

These observations provide valuable insights. Air entrapped within facesheets can migrate towards the core, rather than bag, if P_c is lower than local resin and gas pressures. Fillet formation occurs early, once the adhesive viscosity is sufficiently low. Bond-line porosity can quickly form once the resin

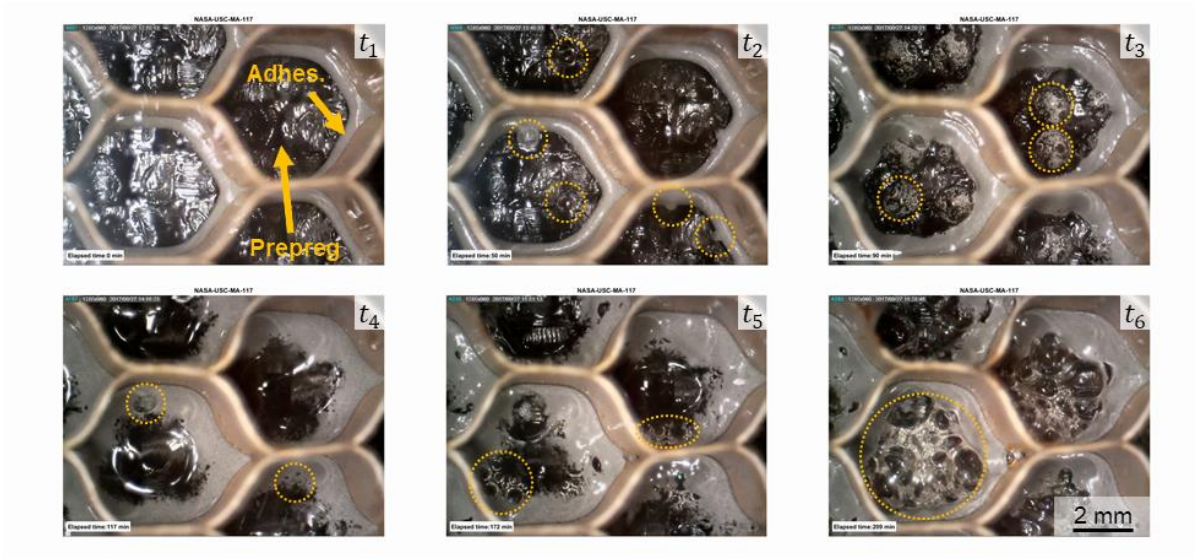

Figure 3: *In situ* observations of bond-line evolution versus time ($t_1 - t_6$).
Key features are indicated in orange.

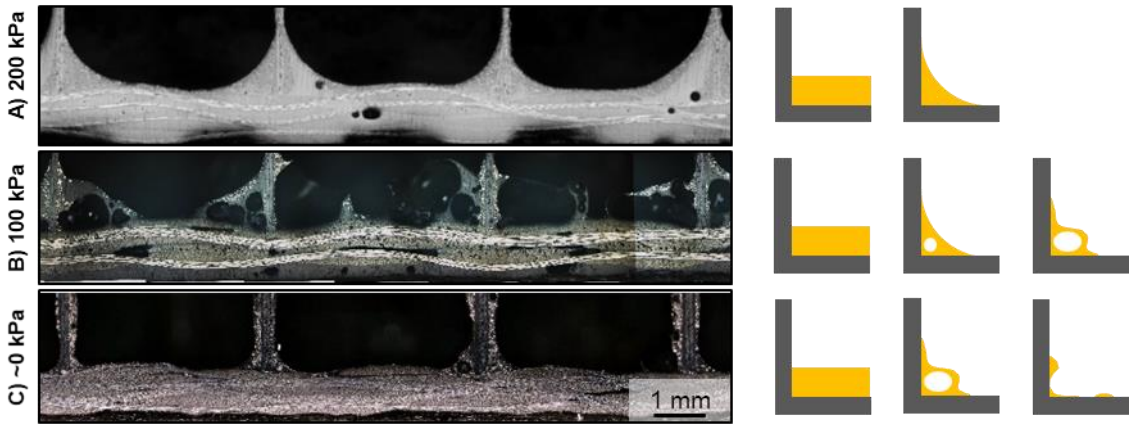

Figure 4: Polished sections of bond-lines cured with P_c of (A) 200 kPa, (B) 100 kPa, and (C) 0 kPa.

viscosity is low, and the size and shape of bubbles can evolve with core pressure. Finally, bond-line porosity can form in *either* adhesive or prepreg resin, depending on driving forces such as concentrations of air, moisture, and other volatilizing species. Critically, this behavior is not restricted to co-cure with reticulated adhesive: other experiments have provided evidence of prepreg resin voids penetrating into the bond-line through pores and cracks in a film adhesive layer. The prepreg used here (HexPly 8552S) is produced using solvent impregnation, and likely contains a volatile ingredient that exacerbates porosity formation at high temperature and low pressure. However, this case study illustrates the potentially important contribution of the facesheet to bond-line quality.

3.2. Challenges: Defect Evolution During Adhesive Bond-Line and Facesheet Formation

The adhesive bond-line formation is both dependent on P_c (as seen in Section 3.1) and path-dependent, and can result in drastically different fillet morphologies. Figure 4 shows polished cross-sections of bond-lines cured with three constant P_c levels. The part co-cured with P_c = 200 kPa (pressurized core) exhibited consistent, well-formed fillets with negligible porosity, and *in situ* observations showed that adhesive flow along cell walls was the only operative phenomena. The part cured with P_c = 100 kPa (ambient pressure) exhibited substantial porosity in fillets because the pressure transferred to the adhesive could not prevent void growth and entrapment at gelation. Finally, the part cured with P_c = 0 kPa (vacuum) exhibited little porosity but small, malformed fillets. For this case, *in situ* visuals showed that, early in the process, large voids grew within the adhesive (or at the interface with the prepreg) and ruptured prior to gelation, redistributing the adhesive onto the cell walls, away from the skin/core interface. These results indicate that core pressure is a critical factor influencing fillet and porosity formation at the bond-line, but also that fillet "quality" does not necessarily vary monotonically with core pressure. Indeed, the potential for void growth and rupture – and, hence, large-scale adhesive redistribution – creates a path-dependecy that complicates process development and control. Indeed, post-redistribution, application of sufficient P_c can collapse voids, but large, uniform fillets can no longer be formed. Fillet formation dynamics are discussed in more details in a separate paper [19].

Prepreg laminate consolidation over core is more challenging than cure over solid tooling. The core substrate is non-uniform, resulting in uneven pressure transfer and allowing resin bleed into core cells. Consolidation phenomena (fiber bed compaction, resin flow, and defect formation) are affected by differences between P_a, P_b, and P_c. Finally, pressure gradients across the skin ($\Delta P/h$, where h is the skin thickness and $\Delta P = P_c - P_b$) can drive gas flow through the prepreg, potentially resulting in porosity. Figure 5 shows a polished cross-section of a co-cured facesheet. Several defects are visible, including inter-ply porosity, compaction variations (with lesser fiber volume fractions over core cells), and dimpling, or displacement of the facesheet into core cells.

Figure 5: Facesheet showing key microstructural features.

Figure 6 shows illustrative results (facesheet porosity and dimpling, both averaged over four polished sections) from a study of facesheet co-cured over core (with film adhesive). The baseline case (I) consisted of four prepreg plies consolidated over core with 3.175 (1/8") cells, under constant P_a = 377 kPa (40 psig) and $P_b = P_c$ = 0 kPa. Porosity of 2.3% and dimpling of 0.13 mm were measured.Case II consisted of modifying the baseline by co-curing with vented bag and core ($P_b = P_c$ = 100 kPa), leading to marginal increases in porosity and decreases in dimpling. Case III consisted of decreasing P_a to 239 kPa (20 psig), and exhibited a marked decrease in porosity. Conversely, in Case IV, further decreasing P_a to 101 kPa (ambient) led to greater porosity but lowest dimpling. Case V related to a thicker facesheet (8 plies, instead of four), with several sections showing notably high porosity. Finally, Case VI consisted of co-cure over larger honeycomb cells (6.35 mm, or 1.4"), and exhibited the greatest extent of dimpling. Standard deviations (and other metrics of dispersion) were high for all averaged data because of significant spatial non-uniformity in co-cured laminates. These results provide insights into defect formation mechanisms during co-cure of prepreg facesheets. The baseline exhibited higher porosity than monolithic laminates made of the same prepreg (which were essentially void-free), indicating that co-cure increases likelihood of defects. Case II shows that simple venting of the vacuum bag is unlikely to enable major improvements in defect levels, and that vacuum-assisted air extraction can be beneficial. Case III indicates that, counter-intuitively, lower P_a levels can reduce porosity levels. This trend is attributed to less resin bleed into the core – and, consequently, decreased resin pressure loss and lower likelihood of resin depletion. However, higher defect levels in Case IV indicate that benefits of low pressure cure are limited, and that OoA/VBO cure may not transfer sufficient pressure. Cases V and VI provide evidence of scale-up challenges to larger geometries. Thicker facesheets render air evacuation more difficult. Larger core cells reduce the areal cell wall density, decreasing the effectiveness of pressure transfer, and subject a larger prepreg area to bending. Overall, these results, and others obtained during this project, indicate that facesheet consolidation over core is significantly more complex than monolithic cure, and that traditional defect control strategies (e.g., increasing the autoclave pressure) can be ineffective (or counterproductive) during co-cure.

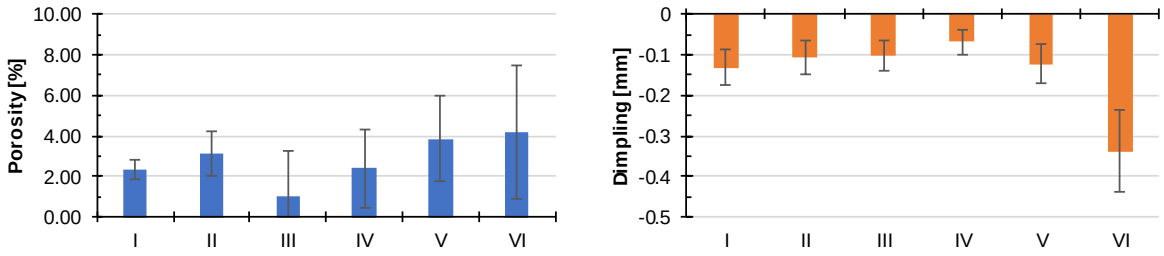

	Facesheet	Core (Cell Size)	Pressure Conditions
I	4 plies	3.175 mm	P_a = 377 kPa, P_b = 0 kPa, P_c = 0 kPa
II	4 plies	3.175 mm	P_a = 377 kPa, **P_b = 100 kPa**, **P_c = 100 kPa**
III	4 plies	3.175 mm	**P_a = 239 kPa**, P_b = 0 kPa, P_c = 0 kPa
IV	4 plies	3.175 mm	**P_a = 100 kPa**, P_b = 0 kPa, P_c = 0 kPa
V	**8 plies**	3.175 mm	P_a = 377 kPa, P_b = 0 kPa, P_c = 0 kPa
VI	4 plies	**6.350 mm**	P_a = 377 kPa, P_b = 0 kPa, P_c = 0 kPa

Figure 6: (A) Porosity and (B) dimpling versus process conditions (listed in table).

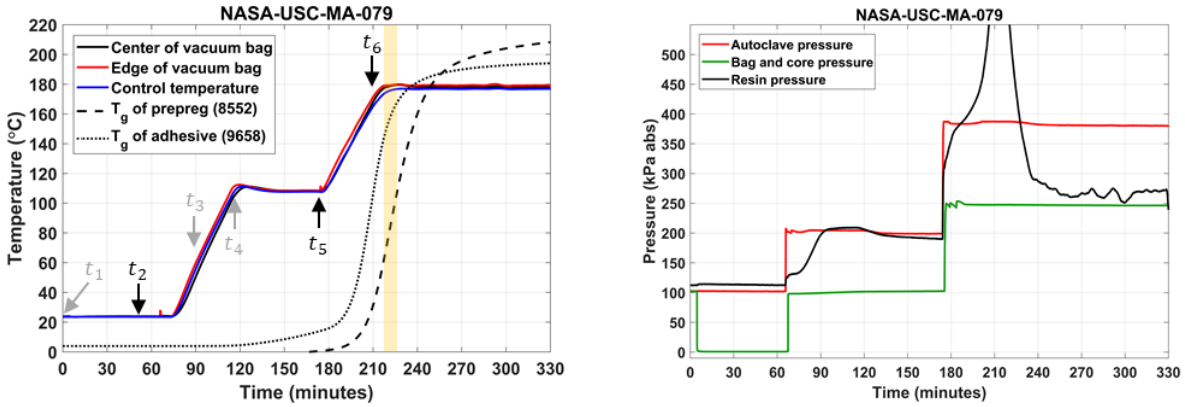

Figure 7: (A) Temperature and (B) pressure data for a co-cure cycle that can achieve defect-free parts.

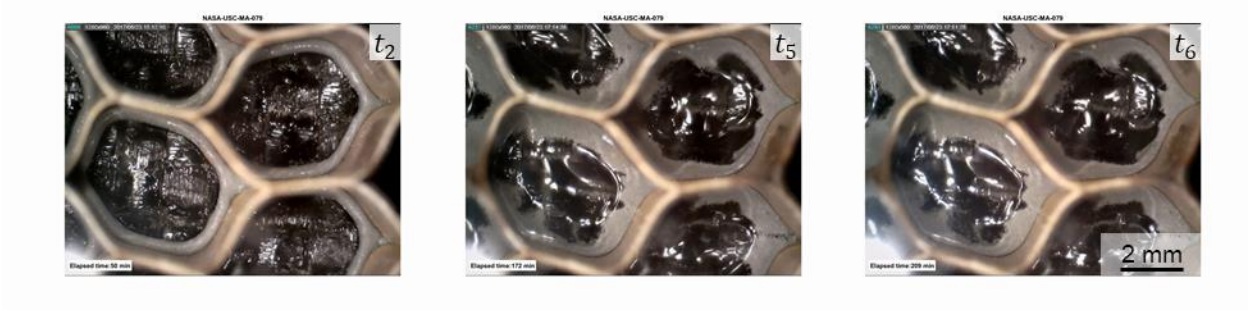

Figure 8: *In situ* observations of bond-line evolution versus time (times t_2, t_5, and t_6).

3.3. Manufacturing Strategy for Defect Control

Defect control strategies for co-cure can be developed by understanding the physics of co-cure and the challenges associated with defect evolution in the bond-line and facesheet. Generally, defect mitigation requires three steps: (1) evacuating entrapped air from facesheets and bond-lines in early stages of co-cure, (2) transferring enough pressure to the prepreg and adhesive to prevent void growth during heated stages, and (3) maintaining necessary pressure levels for the entirety of processing. Honeycomb cores pose the greatest challenge to the third step, because low core pressures and resin bleed into core cells frequently result in pressure losses, even if high autoclave pressures are imposed. The criteria for defect-free parts can be met using in-bag pressurization. Figure 7 displays temperature and pressure data for a successful process trial, while Figure 8 shows video micrographs of the bond-line at three stages of co-cure (t_2, t_5, and t_6). The thermal cycle was identical to that previously used (e.g., Figure 2 and Figure 3). Conversely, a three-stage pressure cycle was devised. First, bag vacuum was drawn at room temperature to remove entrapped air, reducing initial porosity prior to heating. During the first ramp and dwell, P_b and P_c were set to ambient to prevent disruption of the fillets at intermediate temperatures (like in Figure 4C). Finally, during the second ramp and dwell, P_b and P_c were raised to super-ambient levels (239 kPa, or 20 psig) to counteract driving forces for void growth associated with high temperatures and prepreg solvent evolution. Identical P_b and P_c levels were used to preclude gas or resin flow into core or consumables. Furthermore, low consolidation pressures ($P_a - P_b$ = 138 kPa) were imposed to minimize resin bleed by ensuring that resin pressure (P_r) did not greatly exceed P_c. Figure 8 shows that this cycle effectively eliminated void formation in adhesive and prepreg. These results correspond to equilibrated co-cure. However, similar tests have shown that in-bag pressurization is viable for co-cure with a sealed core, so long as the facesheet is sufficiently permeable.

4. Conclusions

This paper describes an extensive research project on the physics of honeycomb sandwich co-cure. *In situ* observations, processing trials, and microstructural analysis were used to understand key phenom-

ena and assess the role of material and process factors on defect formation. Results show that co-cure is governed by interactions between core pressure evolution, bond-line formation, and facesheet consolidation, and that defect evolution is path-dependent and more difficult to control than for monolithic parts. These insights have led to the development of a manufacturing strategy for successful co-cure, which utilizes in-bag pressurization to control bond-line and facesheet defects. Altogether, this work supplies a fundamental scientific basis for understanding honeycomb sandwich co-cure, and addresses a need for optimized and science-based manufacturing processes for advanced composite structures.

Acknowledgments

The authors are thankful for financial support from NASA (NRA NNL16AA13C), material donations from Hexcel, Henkel, Cytec Solvay, The Gill Corporation, and Airtech, and helpful discussions with S. Advani, P. Simacek, N. Niknafs, and T. Cender of the University of Delaware; R. Cano of NASA; S. Amini, W. Zhao, and J. Gangloff of United Technologies; A. Beal of Gill Corporation; and J. Boyd.

References

[1] Hubert, P. and A. Poursartip. Review of flow and compaction modelling relevant to thermoset matrix laminate processing. *Journal of Reinforced Plastics and Composites 17*, 4 (1998), 286–318.
[2] Centea, T., L.K. Grunenfelder, and S.R. Nutt. A review of out-of-autoclave prepregs - material properties, process phenomena and manufacturing considerations. *Composites Part A: Applied Science and Manufacturing 70*, (2015), 132–154.
[3] Tavares, S.S., V. Michaud, and J.A.E. Månson. Through thickness air permeability of prepregs during cure. *Composites Part A: Applied Science and Manufacturing 40*, 10 (2009), 1587–1596.
[4] Tavares, S.S., N. Caillet-Bois, V. Michaud, and J.-A.E. Månson. Non-autoclave processing of honeycomb sandwich structures: Skin through thickness air permeability during cure. *Composites Part A: Applied Science and Manufacturing 41*, 5 (2010), 646–652.
[5] Tavares, S.S., V. Michaud, and J.A.E. Manson. Assessment of semi-impregnated fabrics in honeycomb sandwich structures. *Composites Part A: Applied Science and Manufacturing 41*, 1 (2010), 8–15.
[6] Tavares, S.S., N. Caillet-Bois, V. Michaud, and J.-A.E. Månson. Vacuum-bag processing of sandwich structures: Role of honeycomb pressure level on skin–core adhesion and skin quality. *Composites Science and Technology 70*, 5 (2010), 797–803.
[7] Tavares, S.S., Y. Roulin, V. Michaud, and J.-A.E. Månson. Hybrid processing of thick skins for honeycomb sandwich structures. *Composites Science and Technology 71*, 2 (2011), 183–189.
[8] Kratz, J. and P. Hubert. Processing out-of-autoclave honeycomb structures: Internal core pressure measurements. *Composites Part A: Applied Science and Manufacturing 42*, 8 (2011), 1060–1065.
[9] Kratz, J. and P. Hubert. Anisotropic air permeability in out-of-autoclave prepregs: Effect on honeycomb panel evacuation prior to cure. *Composites Part A: Applied Science and Manufacturing 49*, 0 (2013), 179–191.
[10] Kratz, J. and P. Hubert. Vacuum-bag-only co-bonding prepreg skins to aramid honeycomb core. Part II. In-situ core pressure response using embedded sensors. *Composites Part A: Applied Science and Manufacturing 72*, (2015), 219–227.
[11] Kratz, J. and P. Hubert. Vacuum bag only co-bonding prepreg skins to aramid honeycomb core. Part I. Model and material properties for core pressure during processing. *Composites Part A: Applied Science and Manufacturing 72*, (2015), 228–238.
[12] Levy, A., J. Kratz, and P. Hubert. Air evacuation during vacuum bag only prepreg processing of honeycomb sandwich structures: In-plane air extraction prior to cure. *Composites Part A: Applied Science and Manufacturing 68*, (2015), 365–376.
[13] Kratz, J. and P. Hubert. Evaluation of core material on skin quality for out-of-autoclave honeycomb panels. *Proceedings of the SAMPE 2012 Conference*, Society for the Advancement of Materials and Process Engineering (2012).
[14] Kratz, J., M. Genest, M. Preau, and P. Hubert. Vacuum-bag-only prepreg processing of honeycomb structures: From lab-scale experiments to an aircraft demonstrator. *Proceedings of the SAMPE 2014 Technical Conference*, Society for the Advancement of Material and Process Engineering (2014).
[15] Nagarajan, S., V.G.K. Menta, K. Chandrashekhara, et al. Out-of-Autoclave Sandwich Structure: Processing Study. *SAMPE Journal 48*, 4 (2012), 24–31.
[16] Chen, C., Y. Li, Y. Gu, M. Li, and Z. Zhang. Prediction of the resin fillet size in honeycomb sandwich composites with self-adhesive prepreg skin. *Journal of Reinforced Plastics and Composites 35*, 21 (2016), 1566–1575.
[17] Anders, M., D. Zebrine, T. Centea, and S. Nutt. In-Situ Observations and Pressure Measurements for Autoclave Co-Cure of Honeycomb Core Sandwich Structures. *Journal of Manufacturing Science and Engineering*, (2017).
[18] Anders, M., T. Centea, D. Zebrine, et al. Through-Thickness Gas Permeability of Prepreg Composite Facesheets During Co-Cure of Honeycomb Core Sandwich Structures. *Proceedings of the SAMPE 2018 Technical Conference*, Society for the Advancement of Material and Process Engineering (2018).
[19] Zebrine, D., M. Anders, T. Centea, and S.R. Nutt. Adhesive Bond-Line Formation During Co-Cure of Honeycomb Sandwich Structures. *Proceedings of the SAMPE 2018 Technical Conference (Student Competition)*, Society for the Advancement of Material and Process Engineering (2018).